

DESIGN AND RF TEST OF DAMPED C-BAND ACCELERATING STRUCTURES FOR THE ELI-NP LINAC

D. Alesini, S. Bini, R. Di Raddo, V. Lollo, L. Pellegrino, INFN-LNF, Frascati, Italy; L. Ficcadenti, V. Pettinacci, INFN-Sezione di Roma 1, Rome, Italy; L. Palumbo, University of Rome “La Sapienza”, Italy; L. Serafini, INFN-Sezione di Milano, Italy

Abstract

The linac energy booster of the European ELI-NP proposal foresees the use of 12, 1.8 m long, travelling wave C-Band structures, with a field phase advance per cell of $2\pi/3$ and a repetition rate of 100 Hz. Because of the multi-bunch operation, the structures have been designed with a dipole HOM damping system to avoid beam break-up (BBU). They are quasi-constant gradient structures with symmetric input couplers and a very effective damping of the HOM's in each cell. An optimization of the electromagnetic and mechanical design has been done to simplify the fabrication and to reduce their cost. In the paper we shortly review the whole design criteria and we illustrate the low power RF test results on prototypes that shown the feasibility of the structure realization and the effectiveness of the HOM damping.

INTRODUCTION

An advanced Source of Gamma-ray photons will be built in Magurele (Bucharest, Romania) in the context of the ELI-NP Research Infrastructure [1]. The photons will be generated by Compton back-scattering in the collision between a high quality electron beam and a high power laser. The machine is expected to achieve an energy of the gamma photons tunable between 1 and 20 MeV with a narrow bandwidth (0.3%) and a high spectral density (10^4 photons/sec/eV). The machine is based on a RF Linac operated at C-band (5.712 GHz) with an S-band photoinjector delivering a high phase space density electron beam in the 300-720 MeV energy range. The repetition rate of the machine is 100 Hz and, within the RF pulse, up to 32 electron bunches will be accelerated, each one carrying 250 pC of charge, separated by 16 nsec. The linac booster is composed of 12 TW C-Band disk loaded accelerating structures, each structure, 1.8 m long, is a quasi-constant gradient structure with $2\pi/3$ field phase advance per cell. The main design criteria will be illustrated in the paper with the preliminary RF measurements results.

DESIGN OF THE C-BAND STRUCTURES

The dimensions of each cell of the structures have been optimized to simultaneously obtain: (a) the lowest peak surface electric field on the irises; (b) an average accelerating field of 33 MV/m with an available power from the klystron of 40 MW; (c) the largest iris aperture compatible with the previous points to increase the pumping speed of the structure, to reduce the dipole wakefield intensity and the filling time of the structure

itself. The reduction of this last parameter allows reaching higher accelerating gradient since shorter RF pulse length reduces the breakdown rate.

Since the ELI-NP linac operation is necessarily multi-bunch, in order to achieve the requested photon flux, the structures have been designed with an effective damping of the HOM dipoles modes to avoid BBU instabilities. The solution adopted for the ELI-NP structures is based on a waveguide damping system, similar to the design adopted for the CLIC structures, but the mechanical design has been strongly simplified with respect to CLIC-type structures to reduce the cost and to simplify the fabrication [2]. The main structure parameters are reported in Table 1. Each cell of the structure (shown in Fig. 1) has four waveguides that allows the excited HOMs to propagate and dissipate into silicon-carbide (SiC) RF absorbers. The cells have four tuners and eight cooling pipes to sustain the 100 Hz operation. The SiC tiles have been optimized to avoid reflections and are integrated into the structure. The structure has been designed using ANSYS-HFSS.

Table 1: Main Parameters of the ELI-NP Structures

Structure type	Quasi-Constant gradient
Working frequency (f_{RF})	5.712 [GHz]
Number of cells	102
Structure length	1.8 m
Working mode	TM ₀₁ -like
Iris half aperture radius	6.8 mm-5.78 mm
Cell phase advance	$2\pi/3$
RF input power	40 MW
Average accelerating field	33 MV/m
Acc. field struct. in/out	37-27 MV/m
Average quality factor	8850
Shunt impedance	67-73 MΩ/m
Phase velocity	c
group velocity (v_g/c)	0.025-0.014
Filling time	310 ns
Output power	0.3*Pin
Pulse duration for beam acceleration (τ_{BEAM})	<512 ns
Rep. Rate (f_{rep})	100 Hz
Pulsed heating	<6°C
Average dissipated power	2.3 kW
Working temperature	30 °C

The input and output couplers have a symmetric feeding and rounded edges to reduce the pulsed heating of the surfaces. The input coupler (shown in Fig. 1) integrates a splitter to allow symmetric RF feeding while

the output one has two symmetric outputs connected to two RF load.

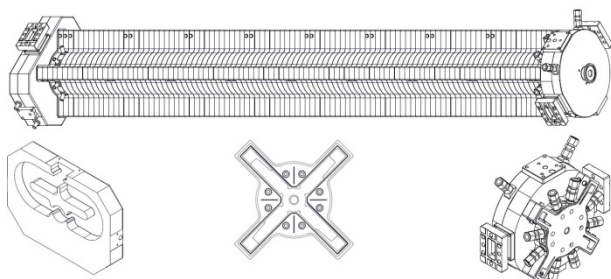


Figure 1: C-Band travelling wave structures.

The input and output couplers have been designed with a race-track shape to completely suppress the quadrupole field components induced by the presence of the waveguide hole apertures. In Fig. 2 there are reported the amplitudes of the multipole magnetic field components [3] in the center of the coupler cells as a function of the race-track thickness. The final coupler race track dimensions have been chosen to completely suppress the quadrupole components in both the input and output couplers: $\Delta x=6.3$ mm and $\Delta x=5.2$ mm for the input and output coupler respectively.

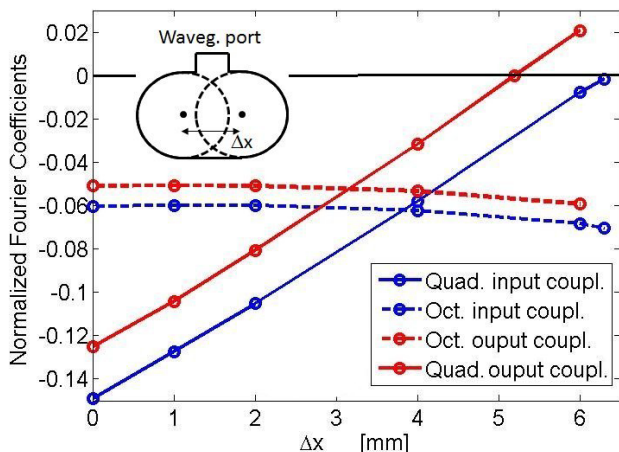


Figure 2: Multipole magnetic field components in the center of the input/output coupler cells.

The structure is fed by a single klystron with a constant RF input pulse and the apertures of the irises have been shaped to have a quasi-constant accelerating field (from 37 to 27 MV/m). It has been decided to adopt such a design with respect to a constant impedance structure because, in this last case, to achieve an average accelerating field of 33 MV/m, the accelerating field in the first cell has to be increased to more than 43 MV/m, giving potential problems from the breakdown rate point of view. On the other hand a perfect constant gradient structure requires very small irises at the end of the structure with a consequent increase of the dipole mode effectiveness, reduction of the pumping speed and beam clearance. The final profile of the accelerating field on axis is given in Fig. 3.

The frequency sensitivity with respect to the cell main parameter is given in Table 2.

A detailed thermal analysis [4] with ANSYS has been done to demonstrate the feasibility operation of the structure under the 100 Hz operation with a 2.3 kW average dissipated power. The temperature distribution along the structure is given in Fig. 4 and the resulting mechanical deformation does not give significant detuning of the structure. Each structure has 14 cooling channels (ID 10 mm): 2 for the input coupler, 2 for the output coupler, 8 for the structure and 2 for the output loads. The total water flow is 66 liter/min. The connections at the end of the tubes are stainless steel fittings, clamped with a metallic seal (e.g. Swagelok two-ferrule design), with the same internal diameter of the tube. The cooling load is 2.3 kW in water, 6 W in air (water temperature 30°C, air temperature 22°C).

Table 2: Frequency Sensitivity with Respect to the Cell Main Parameters

Parameter	Sensitivity ($\Delta f/\Delta par$)
Radius of the cell	-300 kHz/ μ m
Cell iris	70 kHz/ μ m
Cell length	-10 kHz/ μ m
Iris thickness	20 kHz/ μ m

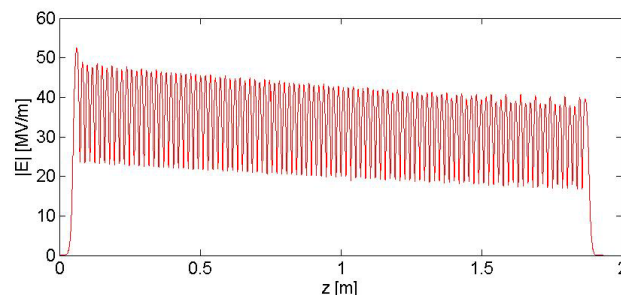


Figure 3: Accelerating field on axis.

At the end of the structure there are two RF loads. Each RF load has one cooling channel with a cooling load of 500 W.

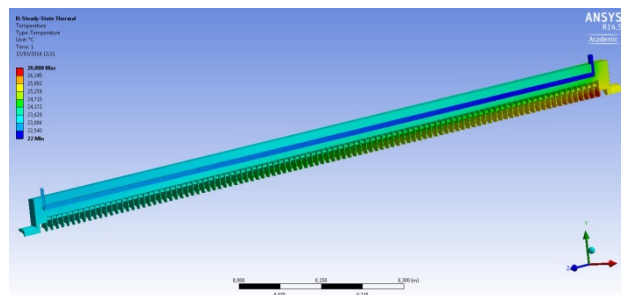


Figure 4: Temperature distribution along the C-Band structure (assuming a water temperature of 22 C).

Vacuum calculations have been performed to evaluate the vacuum pressure along the structure [5]. Two pumping units are foreseen in the structure one at the entrance and one at the end. The pressure profile along the axis of the structure is given in Fig. 5 for two different values of the specific outgassing rate of the copper and of

Content from this work may be used under the terms of the CC BY 3.0 licence (© 2014). Any distribution of this work must maintain attribution to the author(s), title of the work, publisher, and DOI.

the SiC absorbers. In the first case (upper plot) a conservative value of $10^{-12} \text{mbar} \cdot \text{l} \cdot \text{s}^{-1} \text{cm}^{-2}$ has been considered for both copper and SiC while in the second case (bottom plot) a value of $2 \cdot 10^{-14} \text{mbar} \cdot \text{l} \cdot \text{s}^{-1} \text{cm}^{-2}$ and a value of $5 \cdot 10^{-13} \text{mbar} \cdot \text{l} \cdot \text{s}^{-1} \text{cm}^{-2}$ have been considered for copper and SiC respectively. The first values are related to materials without bake-out treatment while the second case to a particular thermal procedure, called vacuum firing, that consists in keeping the structure at 550 Celsius degrees in a vacuum oven for three days at a pressure better than 10^{-7}mbar . Even in the worst case the pressure in the center of the structure is below $8 \cdot 10^{-8} \text{mbar}$ that is sufficient for high gradient operation.

PROTOTYPES AND RF MEASUREMENTS

An intense activity of prototyping has been started to setup and optimize the realization process of the structures. First prototypes have been fabricated to verify both feasibility of copper cells machining and effectiveness of brazing process. We are now focalizing in the realization of two prototypes previous the realization of the first complete structure. The first prototype (“mechanical prototype”) is a full scale device, under construction, without precise internal dimensions conceived to test the full brazing process, verifying structure deformations and vacuum leaks. This prototype does include SiC absorbers to test also the vacuum performances of the structure. The second prototype (“RF prototype”) is a device with a reduced number of cells that we would like to fabricate to test the RF properties of the structure at low and high power. Also this second device includes the SiC absorbers and has precise internal dimensions with tuners.

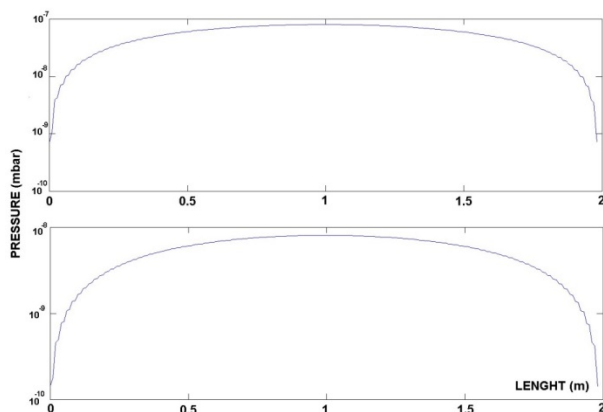


Figure 5: Pressure profile along the axis of the structure for two different values of the specific outgassing rate.

Pictures of a single 12 cell module of the “mechanical prototype” and of the “RF prototype” after brazing are given in Fig. 6. In this last picture the SiC Absorbers are clearly visible. RF test at low power have been performed in the single 12 cell module with and without the SiC absorbers. The results are given in Fig. 7 where the transmission coefficient between two antennas coupled with the structure modes are reported. The measurements

show the effectiveness of the SiC absorbers since the HOM disappear after the insertion of the absorber themselves. The remaining modes are TE-like modes that have a negligible transverse and longitudinal impedance.

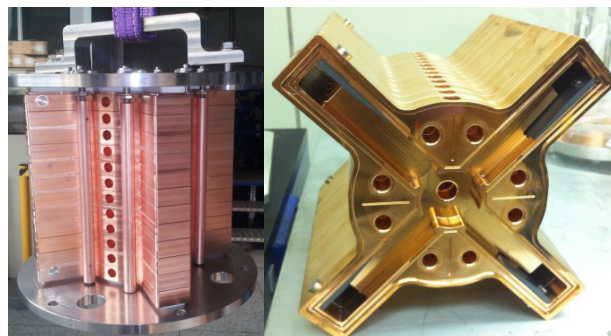


Figure 6: Picture of a single 12 cell module of the “mechanical prototype” after brazing (left) and of the “RF prototype” (right).

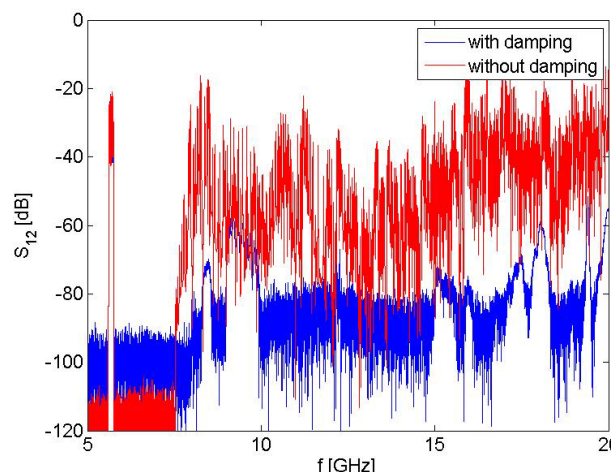


Figure 7: Transmission coeff. between two antennas coupled to a 12 cell module with and w/o the absorbers.

CONCLUSIONS

The linac energy booster of the ELI-NP European proposal foresees the use of 12 travelling wave C-Band structures. In this paper we have illustrated the main design criteria of such structures. An intense prototype activity has been started and is focused on the realization of a first complete structure. First RF measurements have been done and confirm the effectiveness of the SiC absorbers in the damping of the HOM.

ACKNOWLEDGMENTS

We would like to thank P. Chimenti for his technical support in the structure prototype brazing process and F. Pellegrino, A. Mattei (INFN Rome), M. Magi (SBAI Department, “La Sapienza” University, Rome) for their technical support in the “mechanical prototype” production.

REFERENCES

- [1] TDR of ELI-NP Egammas Proposal, under publication, 2014.
- [2] D. Alesini et al., WEPFI013, proc. of IPAC 13, Shanghai, China, 2013.
- [3] D. Alesini, et al., JINST 8 P05004, 2013.
- [4] V. Pettinacci et al., IPAC14, Dresden, Germany, these proceedings.
- [5] S. Bini et al., SPARC-RF-14/001, 2014.